Photoinduced interfacial charge transfer processes in solar photocatalysis degradation of methylene blue using nanostructured ZnO

Hiba K. Wahhab, Zainab F. AL- Bawi, Rawaa A. Faris, Dawood Altiafy

Institute of Laser for Postgraduate Studies, University of Baghdad, Baghdad, Iraq

E-mail: zainabawi@yahoo.com

Abstract

In this research, design of advanced material for sunlight conversion requires focused research to obtain efficient photocatalytic system. Nanostructured ZnO was synthesized using spin coating technique. The structural, morphological and optical properties of annealed nanostructured ZnO thin film at 390 C^o for 3 hours were characterized by x-ray diffraction, atomic force microscope AFM and UV-VIS spectrophotometer. Nanostructured ZnO was applied for removal Methylene Blue (MB) dye from water using sunlight induced photocatalytic process. Overall degradation of MB/ZnO was achieved after 120 minutes of sunlight irradiation while it needs more time for MB alone. The reaction rate constant fit pseudo first order for MB/ZnO degradation was 0.031 min^{-1} compared to 0.018 min^{-1} using blank sample. Annealed nanostructured ZnO thin film was considered as an excellent candidate to enhance photocatalytic system to convert sunlight to chemical energy based on interfacial charges transfer.

عملية نقل الشحنات السطحية المنتجه بواسطة التحلل الشمسي لتفكيك الصبغه الزرقاء باستخدام اوكسيد الزنك النانوي

هبة كاظم وهاب، زينب فاضل مهدي، رواء احمد فارس، داوود عبيد

معهد الليزر للدراسات العليا، جامعة بغداد، بغداد، العراق

الخلاصة

في هذا البحث، من اجل الحصول على نظام تحلل ضوئي كفوء فمن الواجب تركيز البحوث باتجاه تصميم وهندسة مواد متقدمة لتحويل الطاقة الشمسية. فلم اوكسيد الزنك النانوي تم تلدينه بدرجة حرارة 390 درجة مئوية بعد تحضيره باستخدام تقنية الطلاء الدوار. تم فحص التركيب والشكل والخواص البصرية للفلم النانوي الملدن باستخدام جهاز حيود الاشعة السينية، المجهر المكبر الذري ومطياف الاشعه البنفسجيه-المرئية. اضيف فلم اوكسيد الزنك النانوي كمحلل ضوئي لازالة الصبغه الزرقاء من الماء باستخدام اشعة الشمس. اظهرت النتائج ان عملية التفكك الكلي للصبغه الزرقاء في الماء باستخدام اوكسيد الزنك النانوي قد تحققت بعد مرور 120 دقيقه من التشعيع الشمسي بينما يحتاج الى وقت اكثر اذا كانت الصبغه لوحدها. وصل معدل التفاعل الى (0.031) في الدقيقه بينما كان (0.018) في الدقيقه للصبغه لوحدها. وجد ان فلم اوكسيد الزنك النانوي يمكن اعتباره كمرشح ممتاز لتعزيز نظام التحلل الضوئي لتحويل اشعة الشمس الى طاقة كيميائية مبنية على انتقال الشحنات السطحية.

Introduction

Photocatalysis, known as green technique, offers great potential for elimination of toxic chemicals in the environment [1]. Sustainable energy generation for avoiding a future energy crisis depends on pioneering breakthroughs in the design of cost-
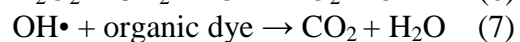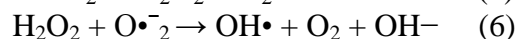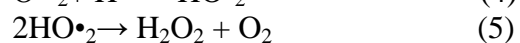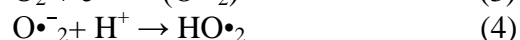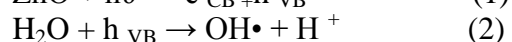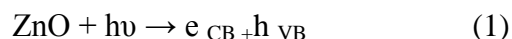
effective and efficient systems for the conversion and storage of energy from renewable sources [2, 3]. Solar-to-chemical energy conversion is one of the most favorable tools to accomplish such demands [4]. In continuation of this, the use of photocatalysts has gained considerable attention because these can be used to convert solar energy to chemical energy.

Metal oxides are widely present in nature and some of them are of great practical use [5]. Zinc oxide (ZnO) are one of these oxides, which are used in many fields [6]. Zinc oxide (ZnO) has stimulated great research interest due to its unique optical and electrical properties that are useful for nanolasers [7], solar cells [8], gas sensors [9, 10], photocatalyst [11, 12]. ZnO-based photocatalytic and photoelectrocatalytic oxidation processes have drawn increasing attention in wastewater treatment because they are non-toxic, chemical and biological stability materials with high photosensitivity [13]. ZnO has been extensively investigated as a semiconductor photocatalyst due to its wide direct band gap (3.2 eV). In the area of water purification, the adaptation of highly advanced nanotechnology offers the possibility of an efficient removal of chemical and biological pollutants. Dyes are presented in many foods and drugs products and have been reported as a possible cause of asthma, urticaria, and angioedema [14]. They are produced in large amounts and enter the water stream during the production and manufacturing processes at different industrial plants. Solar energy is a clean and renewable resource ideal for environmental and sustainable applications. Several works have been published in the photocatalytic process and enhance the efficiency of photocatalysis in nanostructured ZnO due to interfacial charge transfer [15-

17]. Engineering novel useful catalytic systems with nanometer dimensions as a promising friendly solution for environmental remediation using nanostructured ZnO to understand more accurately the interfacial charge transfer on the catalysts surface was achieved.

ZnO photocatalysis for water purification

The photocatalytic activity mechanism of nanostructured ZnO can be described sequencelly starting from Eq. (1) to Eq. (7) [18]. When nanostructured ZnO irradiated with a photon energy ($h\upsilon$) that approximately matches or exceeds its band gap energy (E_g), electron-hole pairs were generated. The electrons can be excited from the valence band (VB) to the conduction band (CB), leaving the same number of holes behind in the VB. Holes can react with water adsorbed molecules to form highly reactive hydroxyl radicals (OH•) as in Eq. (2). Meanwhile, on the surface of the thin films, oxygen trapped the CB-electron to produce superoxide radical ($O{\bullet}^{-}_{2}$) as in Eq. (3). The redox process is based on the interfacial charge transfers (IFCT) which plays a significant role in electron-hole separation considering the energy barriers of the energy level at semicounductor–electrolyte interface. The formed radicals in redox process have a powerful oxidation ability to degrade MB organic dye to produce CO_2 and H_2O as in Eq. (7).

$$ZnO + h\upsilon \rightarrow e_{CB} + h_{VB} \qquad (1)$$
$$H_2O + h_{VB} \rightarrow OH\bullet + H^+ \qquad (2)$$
$$O_2 + e- \rightarrow (O{\bullet}^{-}_{2}) \qquad (3)$$
$$O{\bullet}^{-}_{2} + H^+ \rightarrow HO{\bullet}_2 \qquad (4)$$
$$2HO{\bullet}_2 \rightarrow H_2O_2 + O_2 \qquad (5)$$
$$H_2O_2 + O{\bullet}^{-}_{2} \rightarrow OH\bullet + O_2 + OH^- \qquad (6)$$
$$OH\bullet + \text{organic dye} \rightarrow CO_2 + H_2O \qquad (7)$$

Experimental details
1- Material
Zinc Acetate Dehydrate (ZAD) (Zn (CH$_3$COO)$_2$_2H$_2$O) and Methylene blue dye (C$_{16}$H$_{18}$N$_3$SCl) were supplied from central drug hose, India. The 2-methoxyethanol (C$_3$H$_8$O$_2$) and monoethanolamine (MEA) (C$_2$H$_7$NO) were purchased from Scharlab S.L.Spain.

2- Preparation of photocatalysts
A glass substrate was dipped in the chromic acid to remove organic impurities, then soaked in soap solution to remove any grease present. These slides were then ultrasonically cleaned by distilled water for 10 min each to remove any dust or contaminants present and kept for overnight drying. 0.45 M precursor solution was prepared by dissolving (ZAD) in 2-methoxyethanol and (MEA). Where, they are used as solvent and stabilizer, respectively. 1:1 molar ratio mixture of ZAD to MEA. The mixture was stirred on a hot plate at 65 °C for 1 h until get transparent homogeneous solution. The prepared solution was spun on the pre-cleaned substrates using spin coating technique. In the first 10 s, the spin-speed of the glass substrate was 1500 rpm; in the last 20 s, the spin-speed was 3000 rpm. In order to evaporate the solvent and remove the organic residuals, the films were dried for 5 min after each coating on an open air furnace at 150 °C. The final ZnO thin film was annealed at 390°C for 3 h to obtain crystalline structure. The Michelson interferometer was used to measure the thickness of annealed thin film [19, 20]. The thickness values of annealed ZnO thin film was 294 nm.

3- Characterization techniques
The characterization and structure also the average crystal size of the photocatalyst was measured using Bruker D2 phaser x-ray diffractometer with Cu kα radiation at λ=1.5418 Å. The morphology and the average grain size of annealed nanostructured ZnO thin film were analyzed using atomic force microscopy (AFM, modal AA 3000 scanning probe microscope from angstrom advanced inc., USA). The absorbance spectra of the samples were recorded in the wavelength range 300–1000 nm using a UV–VIS (SHIMADZU 1800) spectrophotometer.

4- Evaluation of photocatalytic activity
The photocatalytic experiments were conducted under ambient atmospheric conditions and at natural pH using sunlight as a light source. All blank MB solution and with nanostructured ZnO catalysts were immersed in a quartz vessel containing the MB solution with concentration (0.019 g/L) as in Fig.1. In order to ensure adsorption/desorption equilibrium, the solution was stirred for about 45 min in dark, prior to the irradiation. The exposure times are (0, 30, 60, 90 and 120) minuets. The absorption spectra were taken after every irradiation exposure time for MB and with annealed nanostructured ZnO thin film catalyst.
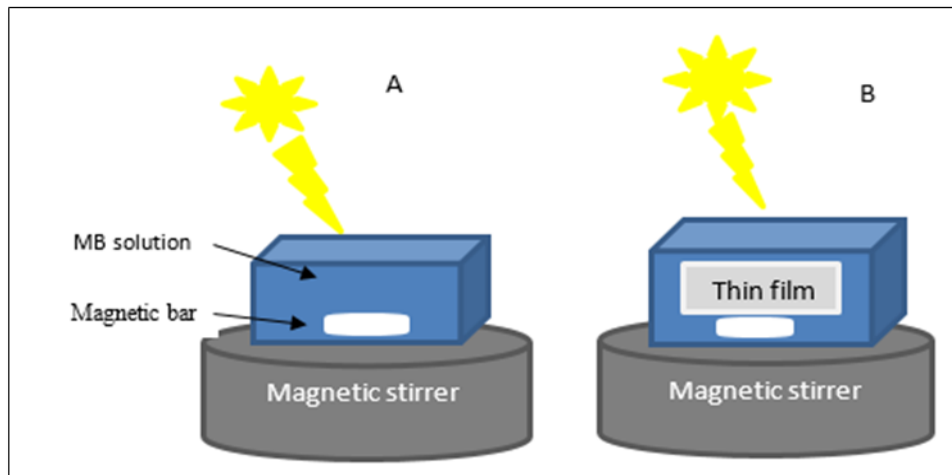
Fig. 1: The experimental schematic for photocatalytic degradation of MB solution (A) MB solution without catalyst (B) MB with nanostructured ZnO thin film.

Results and discussion

1- Structure Analysis of the ZnO thin film

In order to determine the composition of the synthesized annealed nanophotocatalysts, qualitative analysis of XRD patterns was performed for ZnO in Fig. 2. ZnO pattern shows a hexagonal wurtzite with lattice constants (a = b = 3.2299 Å and c= 5.1755 Å), the peaks are consistent with the standard data given in JCPDS cards (JCPDS 36-1451). These results approve the synthesis and immobilization of nanostructured ZnO. In addition, the sharp and intense diffraction peaks are at (100), (002), (101), (102), (110), (103), (200), (112) and (201) phase which is confirmed at 2θ values equal 31.67°, 34.31°, 36.14°, 47.40°, 56.52°, 62.73°, 66.28°, 67.91° and 69.03°, respectively. There is no evidence of bulk remnant materials and impurities. From the spectrum, the average crystalline size of the ZnO is 23 nm. The photocatalytic activity of the system increases dramatically with decreases crystalline size due to increase surface-to-volume ratio. A significant fraction of the atoms (or molecules) in such systems are surface atoms that can be gained surface reactions.
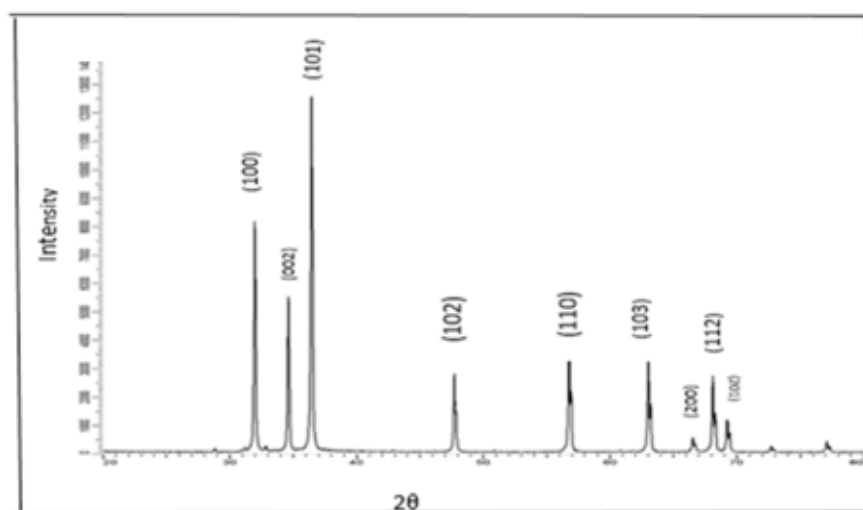

Fig. 2: X-Ray diffraction pattern of ZnO thin film.

The dislocation density (δ) is 20.66 $\times 10^{-4}$ (nm)$^{-1}$ which represents the amount of defects in the sample is defined as the length of dislocation lines per unit volume of the crystal and was calculated using the Eq. (8) [21]:

$$\delta = 1 / D^2 \qquad (8)$$

where D is the crystallite size.

The lattice strain 'ϵ' value of annealed nanostructured ZnO thin film calculated from all XRD peaks was 0.0019 as in Fig. 3. That means the nanostructured ZnO sample was purity crystalline with little amount of defects and had a weak hardness. Therefore, it can be suggested that annealing method is an effective method to repair the structural defects of the ZnO sample. Where, the defects can become the recombination center of the photogenerated charges and thus worsen the photocatalytic activity. So, the high purity of nanostructured ZnO can be improved the photocatalytic activity.
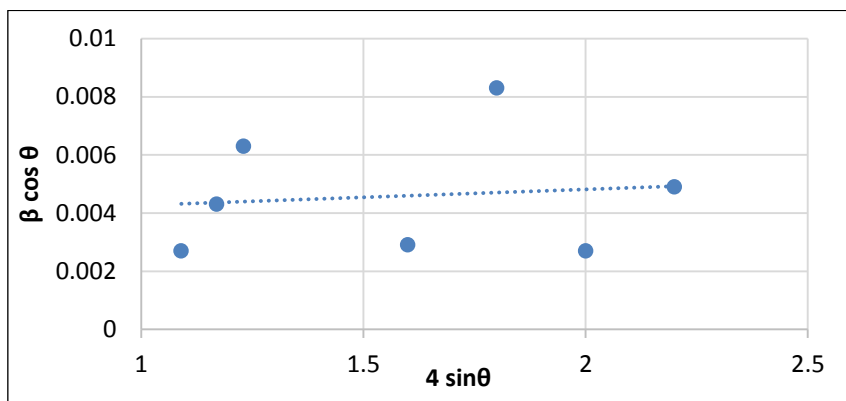

Fig. 3: The strain of nanostructured ZnO.

2- Morphological analysis

The topological properties of annealed nanostructured ZnO thin film done by AFM is shown in Fig. 4. The average grain size was 79.25nm and the surface roughness was equal to 1.22 nm. This figure shows that the morphology of the thin film has a large number of grain size with a circle-shape and are quasi-homogeneously distributed, which indicates the crystalline nature of the films. From the granularity distribution charts, the distribution of particles size were Gaussian curve in range between 40 and 120 nm.
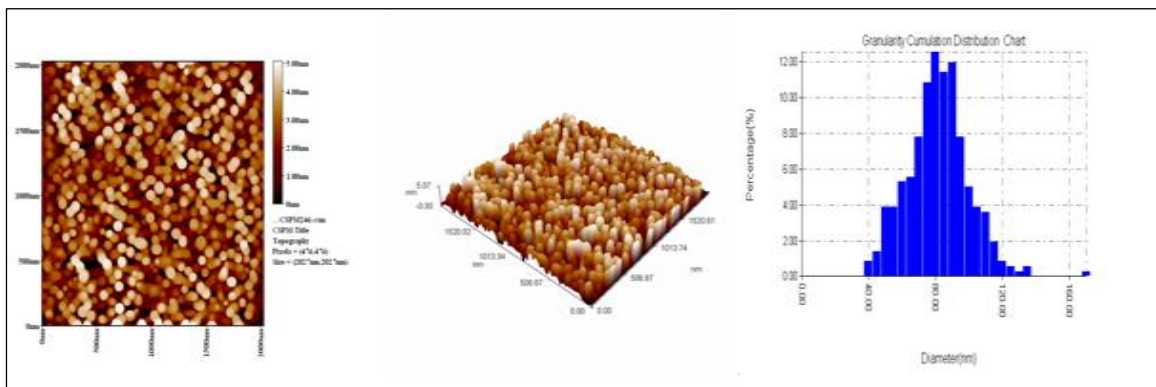

Fig. 4: 2D, 3D images and granularity distribution chart of the atomic force microscopy for the nanostructured ZnO thin film.

3- The optical properties of nanostructured ZnO

Fig. 5 shows the absorption spectra of the nanostructured ZnO thin film before and after annealing in the UV region and almost all the visible spectrum radiations are transmitted. At the annealing temperature, the optical absorption edge is higher and slightly shifted towards the longer wavelength according to change in their morphologies, particle size and surface microstructures with the annealing temperature. The band gap of ZnO was 3.4 eV before the annealing process while it decreased to 3.2 eV after annealing. From these results, diminishing in the band gap could be occurred because of the appearance of band tail resulting from defects associated with the presence of cavities and surface roughness. It was known that during thermal annealing at temperature below the glass transition temperature Tg, the unsaturated defects are gradually annealed producing a larger number of saturated bonds. The reduction in the number of unsaturated defects decreases the density of localized states in the band structure. The wide band gap is necessary to enhance photocatalytic activity. Nevertheless, narrow band gap semiconductor is difficult to maintain photoactivity over a long period of time due to the fast recombination of photogenerated electron–hole pairs.
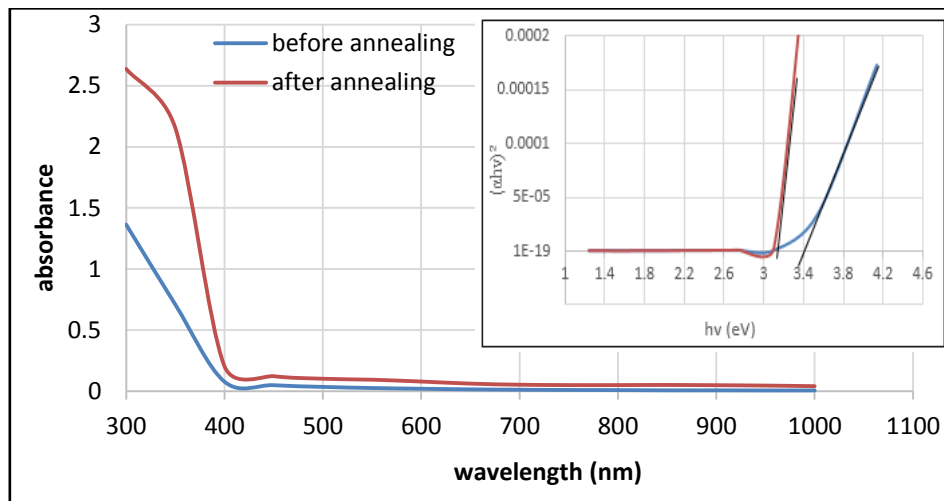

Fig. 5: The absorption spectra of nanostructured ZnO thin film and its band gab after and before annealing process.

4- Photocatalytic degradation of methylene blue dye under sunlight illumination

At blank experiment, UV-VIS absorption spectra for the direct photolysis of MB dye is presented in Fig. 6. UV-VIS absorption spectra of the degradation MB dye using annealed nanostructured ZnO thin film is presented in Fig. 7. According to the change of the absorbance intensity at 664 nm, the completely decolorization of MB solutions was observed after 120 min of irradiation by sunlight. UV irradiation which reaches to the nanophotocatalyst surface leads to form the hydroxyl radicals •OH and O•$_2^-$ anions. These reactive radicals can be degraded the MB dye. From the figure, the results indicated that both of the irradiation and nanostructured ZnO photocatalyst were necessary for the effective removal of the MB where the blue solution of dye transforms to transparent and more light can get through it.
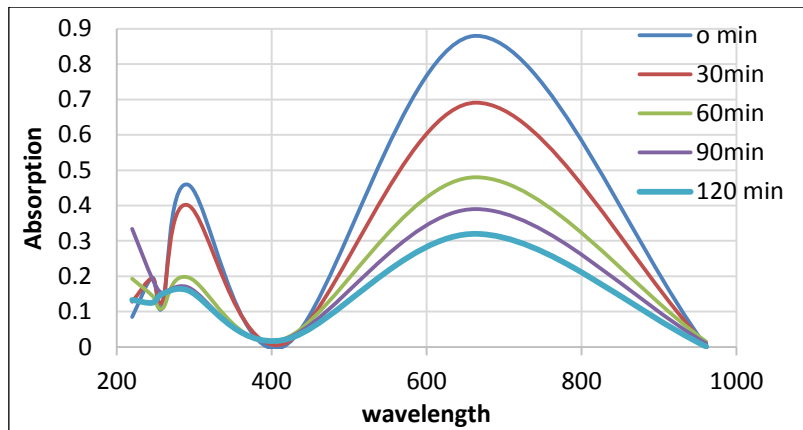
Fig. 6: Absorption spectra of MB dye without catalysis under sunlight irradiation.
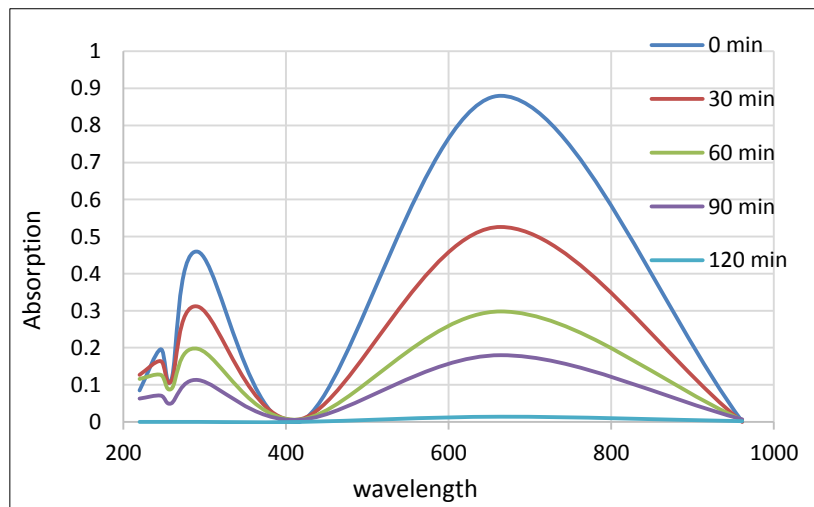

Fig. 7: Absorption spectra of MB solutions with nanostructured ZnO under sunlight irradiation.

The photocatalytic degradation process obeys first pseudo order kinetics that is defined as:

$$-\ln C_t / C_0 = k_a\, t \qquad (9)$$

where, C_0 is the initial concentration, C_t is the reaction concentration of MB, k_a is a pseudo–first-order rate constant and t is an irradiation time [22]. By plotting the $-\ln (C_t/C_0)$ versus sunlight irradiation time as shown in Fig. 8, one can get the value of rate constant k_a which is equal to the slope. The values of a pseudo–first-order (rate constant) k_a are equal to 0.031 for nanostructured ZnO and 0.018 min^{-1} for blank. Therefore, the photodegradation efficiency with nanostructured ZnO is approximately two times greater than the self-degradation of the MB solution under sunlight irradiation.
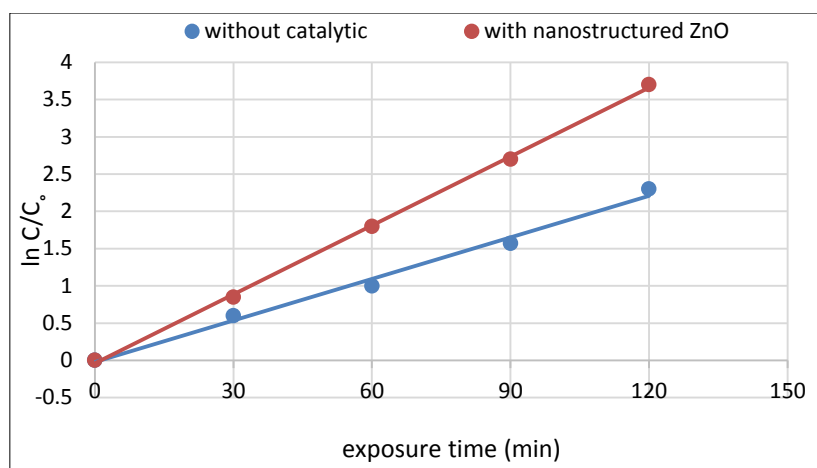
Fig. 8: Determination the pseudo-first-order kinetic rate constants for blank MB solution and with nanostructured ZnO.

Conclusions

In this work, efficient ZnO nanocatalysts was prepared at certain thickness which offer possibilities for finding an appropriate environmentally friendly solutions for transform sunlight into chemical energy more efficiently. The photocatalyst activity of nanostructured ZnO is approximately twice than the direct photolysis of the MB solution under sunlight irradiation. The enhancement of photocatalytic performance using annealed nanostructured ZnO is due to efficient interfacial electron transfer.

References

[1] M.R. Hoffmann, S.T. Martin, W. Choi, D.W. Bahnemannt, Environmental Applications of Semiconductor Photocatalysis. Chem. Rev., 95 (1995) 69-96

[2] M. Jefferson, Renew. Energy, 31 (2006) 571-582.

[3] N. H. Afgan, D. Al Gobaisi, M. G. Carvalho, M. Cumo, Renew. Sustain. Energy Rev., 2 (1998) 235-286.

[4] M. G. Walter, E. L. Warren, J. R. McKone, S. W. Boettcher, Q. Mi, E. A. Santori, N. S. Lewis, Chem. Rev., 110 (2010) 6446-6473.

[5] Aysar A. Alamery, Zainab F. Mahdi, Hussein A. Jawad American Journal of Mechanical Engineering, 3 (2015) 21-25.

[6] Adel K. Mahmoud, Fadhil Z., Suha I. Anissa, International Congress Machines, Tchnologies, Materialss, 22 (2015) 51-56.

[7] M.H. Huang, S. Mao, H. Feick, H.Q. Yan, Y.Y. Wu, H. Kind, E. Weber, R. Russo, P.D. Yang, Science, 292 (2001) 1897-1899.

[8] O. Kluth, G. Schöpe, J. Hüpkes, C. Agashe, J. Müller, B. Rech, Thin Solid Films, 442 (2003) 80-85.

[9] N.J. Dayan, S.R. Sainkar, R.N. Karekar, R.C. Aiyer, Thin Solid Films, 325 (1998) 254-258.

[10] P. Mitra, A.P. Chatterjee, H.S. Maiti, J. Mater. Sci., 9 (1998) 441-445.

[11] E.S. Jang, J.H. Won, S.J. Hwang, J.H. Choy, Adv. Mater., 18 (2006) 3309-3312.

[12] C.H. Ye, Y. Bando, G.Z. Shen, D.J. Golberg, Phys. Chem., B 110 (2006) 15146-15151.

[13] Y.X. Wang, X.Y. Li, G. Lu, X. Quan, G.H. Chen, J. Phys. Chem., C 112 (2008) 7332-7337.

[14] Konstantinou IK, Sakellarides TM, Sakkas VA, Albanis TA, Environ. Sci. Tech., 35 (2001) 398-405.

[15] G.T. Delgado, C.I.Z. Romero, S.A.M. Hernández, R.C. Pérez, O.Z. Angel, Sol. Energy Mater. Sol. Cells, 93 (2009) 55-59.

[16] F.M. Meng, X.P. Song, Z.Q. Sun, Vacuum, 83 (2009) 1147-1151.

[17] J. Xu, Y.G. Chang, Y.Y. Zhang, S.Y. Ma, Y. Qu, C.T. Xu, Appl. Surf. Sci., 255 (2008) 1996-1999.

[18] Yamina Ghozlane Habba, Martine Capochichi-Gnambodoe, Linda Serairi, and Yamin Leprince-Wang, Phys. Status Solidi, B, (2016) 1-5.

[19] Alia'a M. Yahya, Zainab F. Mahdi, Rawaa A. Faris ,Ghuson H. Mohammed, Chemistry and Materials Research, 6, 2 (2014) 47-54.

[20] Yuanxing Fanga, Wei Cheat Leea, Giacomo E. Canciani, Thomas C. Draper, Zainab F. Al-Bawi, Jasbir S. Bedi, Christopher C. Perry, Qiao Chena, Materials Science and Engineering B, 202 (2015) 39-45

[21] VD Mote, Y. Purushotham, BN Dole, Journal of Theoretical and Applied Physics, 6, 6 (2012) 1-8.

[22] Mohammed A. Gondal, Mohammad N. Sayeed, Journal of Environmental Science and Health Part A, 43 (2008) 70-77.